Acta Crystallographica Section D
Biological Crystallography
ISSN 0907-4449

Structure of *Haemophilus influenzae* HslV protein at 1.9 Å resolution, revealing a cation-binding site near the catalytic site

Marcelo C. Sousa* and David B. McKay

Department of Structural Biology, Stanford University School of Medicine, Stanford, CA 94305, USA

Correspondence e-mail: dave.mckay@stanford.edu

Received 11 July 2001
Accepted 25 September 2001

PDB References: HslV (Na^+), 1g3k; HslV (K^+), 1jjw.

The structure of the *Haemophilus influenzae* HslV protease of the HslUV 'prokaryotic proteasome' has been solved by molecular replacement and refined with data to 1.9 Å resolution. The protease is a 'double donut' of hexameric rings; two alternative sets of intermolecular interactions between protomers in the rings result in 'quasi-equivalent' packing within the assembly. Anomalous scattering data from crystals with potassium present in the mother liquor reveal a K^+ ion bound with octahedral coordination near the active-site Thr1 residue. The site also binds Na^+ ions and is likely to bind Mg^{2+}, suggesting that monovalent and divalent metal ions may influence the catalytic activity of the protease.

1. Introduction

The HslV protease is a homolog of the catalytic subunits of the eukaryotic proteasome (Chuang *et al.*, 1993). Protomers of HslV assemble into a dodecamer as a 'double donut' of two hexamers, with a large interior cavity that houses the active sites (Kessel *et al.*, 1996; Rohrwild *et al.*, 1997). By itself, the HslV protease has minimal peptidase activity on either small peptide substrates or large polypeptide/protein substrates. The peptidase activity is enhanced by one to two orders of magnitude when the molecular chaperone HslU binds HslV (Huang & Goldberg, 1997; Seol *et al.*, 1997; Yoo *et al.*, 1997). In addition to allosterically activating the peptidase activity upon binding, HslU recruits, unfolds and translocates protein substrates to the interior cavity of HslV for degradation.

The structure of the *Escherichia coli* HslV protease was initially reported at 3.8 Å resolution (Bochtler *et al.*, 1997) and more recently was reported at 2.8 Å resolution in crystals containing both HslV and HslU (Bochtler *et al.*, 2000). These structures revealed the similarity of the tertiary folds of HslV and the catalytic subunits of the archaeal (Löwe *et al.*, 1995) and yeast (Groll *et al.*, 1997) proteasomes. The structure of a complex between the HslV and HslU proteins of *H. influenzae* has been reported at 3.4 Å resolution, revealing the conformational changes induced in HslV by the HslU chaperone that may be responsible for enhancing the peptidase activity (Sousa *et al.*, 2000). An alternative complex between *E. coli* HslV and HslU, which does not show similar conformational changes, has been reported at 3.0 Å resolution (Wang *et al.*, 2001).

The limited resolution of these structures precludes precise definition of molecular interactions and conformation and also of solvent and metal-ligand structure. Here, we report the structure of the *H. influenzae* HslV protease, which shares 81% sequence identity with its *E. coli* counterpart, at 1.9 Å resolution. The refined models, in combination with anomalous scattering data, reveal a monovalent ion-binding site in proximity to the catalytic site of HslV. In addition, in this particular crystal form the *H. influenzae* HslV dodecamer provides an example of 'quasi-equivalent' oligomer assembly, which results from two alternative sets of protomer–protomer packing interactions within the hexameric rings.

2. Experimental

2.1. Protein expression, purification and crystallization

Recombinant *H. influenzae* HslUV protein (a complex between HslV and HslU) was expressed in *E. coli* and purified as described in Sousa *et al.* (2000). Crystals of HslV were grown at 277 K in hanging drops from solutions of HslUV (20 mg ml^{-1} in 5 m*M* $MgCl_2$, 1 m*M* ADP, 10 mM MOPS pH 7.0) using a precipitant containing 30% polyethylene glycol of average molecular weight 400 (PEG 400), 100 m*M* sodium citrate, 100 m*M* Tris–HCl pH 8.5 and stabilized in the same precipitant solution (the 'Na^+ mother liquor'). SDS–PAGE of redissolved crystals confirmed

Table 1
Crystallographic data-collection and refinement statistics.

Space group *I*222. Values in parentheses are for the last resolution shell.

	HslV (Na^+)†	HslV (K^+)
Data collection		
Unit-cell parameters (Å)	a = 79.02, b = 121.80, c = 126.18	a = 78.89, b = 122.33, c = 126.29
Wavelength (Å)	0.98	1.55
Resolution range (Å)	30–1.90 (1.97–1.90)	30–1.90 (1.97–1.90)
Observations		
Total	229553 (>17867)‡	289305 (>19795)‡
Unique	48345 (4815)	46472 (4693)
Completeness (%)	99.9 (100.0)	96.4 (98.3)
Average $I/\sigma(I)$	28.2 (7.3)	28.8 (9.1)
R_{sym}§	0.057 (0.179)	0.049 (0.195)
Refinement		
Resolution range (Å)	30–1.90 (1.97–1.90)	30–1.90 (1.97–1.90)
R_{cryst}¶	0.200 (0.224)	0.217 (0.258)
R_{free}	0.230 (0.253)	0.251 (0.334)
No. of reflections (working set)	43363	80086††
No. of reflections (test set)	4870	8730
No. of protein atoms	3835	3847
No. of solvent/hetero atoms	198/3 (Na^+)	191/3 (K^+)
Average B value, main-chain atoms (Å^2)	23.9	33.3
Average B value, all atoms (Å^2)	25.7	34.9
R.m.s.d. bond length (Å)	0.010	0.009
R.m.s.d. angles (°)	1.60	1.48

† Data-collection and refinement statistics for the Na^+ structure have previously been included as appendix material in Sousa *et al.* (2000). ‡ Lower bound on number of observations in last shell estimated from *SCALEPACK* output, which gives ranges of number of observations for reflections at higher redundancy (*e.g.* 5–6, 7–8, 9–12). § $R_{sym} = \sum |I_{hkl} - \langle I_{hkl}\rangle| / \sum \langle I_{hkl}\rangle$, where I_{hkl} is a single value of the measured intensity of the *hkl* reflection and $\langle I\rangle$ is the mean of all measured intensities of the *hkl* reflection. ¶ $R_{cryst} = \sum |F_{obs} - F_{calc}| / \sum F_{obs}$, where F_{obs} is the observed structure-factor amplitude and F_{calc} is the structure factor calculated from the model. R_{free} is computed in the same manner as R_{cryst}, using the test set of reflections. †† Includes both reflections of Bijvoet pairs.

that they contained only HslV, despite growing from a protein solution that contained both HslU and HslV.

2.2. Data collection and structure determination

For data collection, crystals were taken directly from the crystallization solution and flash-frozen in a stream of nitrogen gas at ~100 K. To replace Na^+ with K^+, the sodium citrate in the stabilization solution was replaced with potassium citrate in four equal increments of fractional concentration. The crystals are orthorhombic, space group *I*222, with three HslV protomers per asymmetric unit. Crystallographic data were collected from the Na^+-containing crystals on beamline 9-1 of the Stanford Synchrotron Radiation Laboratory (SSRL) using a wavelength of 0.98 Å and from the K^+-containing crystals on SSRL beamline 9-2 using a wavelength of 1.55 Å to enhance the anomalous signal of potassium ($f'' \simeq 1.08$ at 1.55 Å; Cromer, 1974). Raw intensity data were processed and scaled with *DENZO*/*SCALEPACK* (Otwinowski & Minor, 1997). Crystal parameters and data-collection statistics are summarized in Table 1.

The structure of *H. influenzae* HslV with Na^+ was solved by molecular replacement using a protomer of the 3.8 Å resolution *E. coli* HslV structure as a search model. The *E. coli* and *H. influenzae* HslV proteins share 81% sequence identity; non-identical residues were replaced with alanine. The molecular-replacement solutions were subjected to rigid-body refinement using the program *CNS* and an $F_o - F_c$ map calculated to 2.5 Å. Many of the truncated side chains were visible in all three HslV protomers, confirming the correctness of the solutions. A round of Cartesian simulated annealing clarified most of the remaining side chains. After rebuilding, the model was subjected to three rounds of positional and atomic *B*-factor refinement using data to 1.9 Å. Many solvent molecules became apparent and were added into the model. Several cycles of manual rebuilding followed by positional and atomic *B*-factor refinement were carried out until no further improvement in the free *R* factor was observed. Final refinement statistics are summarized in Table 1. The structure of HslV with K^+ was solved using the isomorphous HslV with Na^+ as a starting model. An anomalous difference Fourier confirmed the identity of the monovalent ion. Molecular-replacement calculations were effected with the program package *AMoRe* (Navaza, 1994), refinement was performed with *CNS* (Brunger *et al.*, 1998) and model building was carried out with *O* (Jones *et al.*, 1991).

2.3. Comparison of HslV protomers

Transformations which superimpose one HslV protomer on another were computed with the program *LSQMAN* from the Uppsala Software Factory (Kleywegt & Jones, 1997). The surface area of interaction between HslV protomers was computed with a probe radius of 1.4 Å using the method of Lee & Richards (1971) as implemented in *CNS* (Brunger *et al.*, 1998). The percentage of interaction area that was polar *versus* non-polar was estimated in the same manner after non-polar or polar residues at the interface were deleted from the coordinate files.

2.4. Peptide hydrolysis activity assay

Peptide hydrolysis activity was assayed as described previously (Sousa *et al.*, 2000). Briefly, assays were carried out at 298 K in 3 ml of a solution containing 4 µg ml^{-1} HslUV, 0.1 m*M* benzyloxycarbonyl-Gly-Gly-Leu-7-amido-4-methylcoumarin (Z-Gly-Gly-Leu-AMC; Bachem), 5 m*M* $MgCl_2$, 25 m*M* Tris–HCl pH 7.8, 1 m*M* ATP and 150 m*M* KCl or 150 m*M* NaCl. The release of AMC produced by peptide hydrolysis was followed by continuously monitoring the fluorescence with an excitation wavelength of 380 nm and an emission wavelength of 430 nm.

3. Results and discussion

The HslV crystals have three protomers per asymmetric unit, packed in a manner in which applying the symmetry operations of two perpendicular crystallographic twofold axes generates the 'double donut' of two hexameric rings that is observed in solution. The model includes all amino-acid residues except the carboxy-terminal asparagine residue, one monovalent ion and ~65 H_2O molecules for each of the three independent protomers. The coordinate errors estimated by the method of Luzzati (1952) are 0.22 and 0.24 Å for the structures with Na^+ and K^+, respectively. When the HslV subunits are superimposed on each other, the average r.m.s. differences in backbone atomic positions are 0.46, 0.56 and 0.32 Å for the *AB* pair, the *AC* pair and the *BC* pair, respectively. Superposition of the *H. influenzae* HslV protomers on the protomers of *E. coli* HslV (Bochtler *et al.*, 2000) gives values in the range 0.9–1.0 Å for r.m.s. differences in positions of backbone atoms.

3.1. Quasi-equivalent subunit interactions in the HslV hexamer

The hexameric rings of HslV are notably oblong and deviate from sixfold rotational symmetry owing to 'quasi-equivalent' subunit packing (Fig. 1). As one illustration of the asymmetry, the nearest $C_\alpha-C_\alpha$ distance across the central pore between subunits *A* and *A*′ (cyan in Fig. 1*a*) is 25.7 Å, while the equivalent distance between subunits *C* and *C*′ (gold in Fig. 1*a*) is 13.1 Å. The buried surface area of interaction between pairs of subunits in the hexameric ring is ∼1600, ∼1400 and ∼800 Å^2 for the *AB*, *BC* and *CA*′ subunit interfaces, respectively. In each case, the interface area is divided approximately equally between polar and non-polar interactions. The angular rotation around the pseudo-sixfold axis that superimposes the *A* protomer on *B* is 60.3°. The rotation components of the transformations that superimpose *B* on *C* and *C* on *A*′ are 58.5 and 63.3°, respectively. (The three angles do not sum to exactly 180° because the axes of the transformations are not precisely along the pseudo-sixfold.) Thus, although HslV forms a stable dodecamer in solution, the interactions between subunits within the dodecamer are apparently quite malleable.

The most notable differences in intersubunit contacts are seen in the ionic interactions between the apical helices, which lie on the exterior of the dodecamer. In the interface between subunits *A* and *C* (Fig. 1*b*), Lys80 and Arg83 from subunit *A* make salt bridges with Glu58 of subunit *C*. The guanidinium group of Arg83 is stabilized by its interaction with the carboxyl group of Asp111, whose side-chain orientation is in turn dictated largely by the conformation of the neighboring Gly110, whose Ramachandran angles are $(\varphi, \psi) = (-113, 18°)$.

A different set of interactions arise between subunits *B* and *C* (Fig. 1*c*). In subunit *C*, Gly110 adopts an alternative conformation with $(\varphi, \psi) = (77, 22°)$. As a consequence, the side chain of Asp111 is oriented differently and does not interact with Arg83. Arg83 of subunit *C* makes a salt bridge with Asp52 of subunit *B*, while Lys80 forms an intra-helix salt bridge with Glu77. The third set of pairwise interactions between subunits, between *A* and *B*, are similar to those between *B* and *C*, with slightly different interatomic distances. The conformation of Gly110 in subunit *B* is similar to that of subunit *C*, with $(\varphi, \psi) = (69, 29°)$. When the hexameric HslU chaperone binds HslV, the apical helices are shifted substantially and the carboxy terminal peptide of HslU intercalates between HslV subunits (Sousa *et al.*, 2000). In the HslUV complex, the ionic interactions between the apical helices of HslV are similar to those between the *AB* pair and the *BC* pair in the HslV structure presented here.

3.2. Ion-binding site in HslV

During model refinement of the Na^+-containing structure, the surrounding ligand environment of one solvent peak displayed a geometry that was inconsistent with a H_2O molecule, but consistent with a Na^+ ion (Glusker, 1991). Presence of a monovalent ion at this site was confirmed by a peak in an anomalous difference Fourier on data collected on K^+-containing crystals (Fig. 2). In the two structures, both ions are bound with a distorted octahedral geometry; three ligands are provided by the carbonyl O atoms of residues 157, 160 and 163, and the remaining three ligands are the O atoms of H_2O molecules. The average ion–oxygen distance for the carbonyl O atoms is 2.3 Å for the Na^+ ion and 2.6 Å for the K^+ ion; the average ion–oxygen distances for the H_2O molecules are 2.5 and 2.8 Å for Na^+ and K^+, respectively. The bound Na^+ and K^+ ions are ∼11 Å from the catalytic hydroxyl group of Thr1, precluding a direct participation in the hydrolytic mechanism. However, hydrogen-bonding interactions link the metal-ion binding loop to the active-site threonine; specifically, the carbonyl group of Phe162 as well as the hydroxyl group of Ser125 are within hydrogen-bonding distance of the main-chain amino group of Thr1, suggesting that they function to constrain the amino-terminal threonine residue to a conformation in which the hydroxyl is in an orientation that is favorable for the hydrolysis of substrates.

The yeast proteasome has Mg^{2+} bound in equivalent sites of some subunits (Groll *et al.*, 1997). Specifically, the proteasome is a 28-subunit assembly with two identical rings of seven β-subunits that form a double donut and two identical rings of seven α-subunits bound distally on each β-subunit. Three of the seven β-subunits (β1, β2 and β5) are catalytically active; each of these has an Mg^{2+} ion bound at this site with octahedral coordination. In addition, two inactive β-subunits bind Mg^{2+} ions at sites adjacent to those of active subunits, thereby forming a magnesium-mediated '*β-trans-β*' linkage between the subunits (β6′ to β2 and β3′ to β5, where the prime denotes the second ring), whereby one of the ligands is an O atom of the main-chain carboxy terminus of a neighboring subunit. None of the α-subunits have Mg^{2+} bound at the equivalent site, despite their close similarity

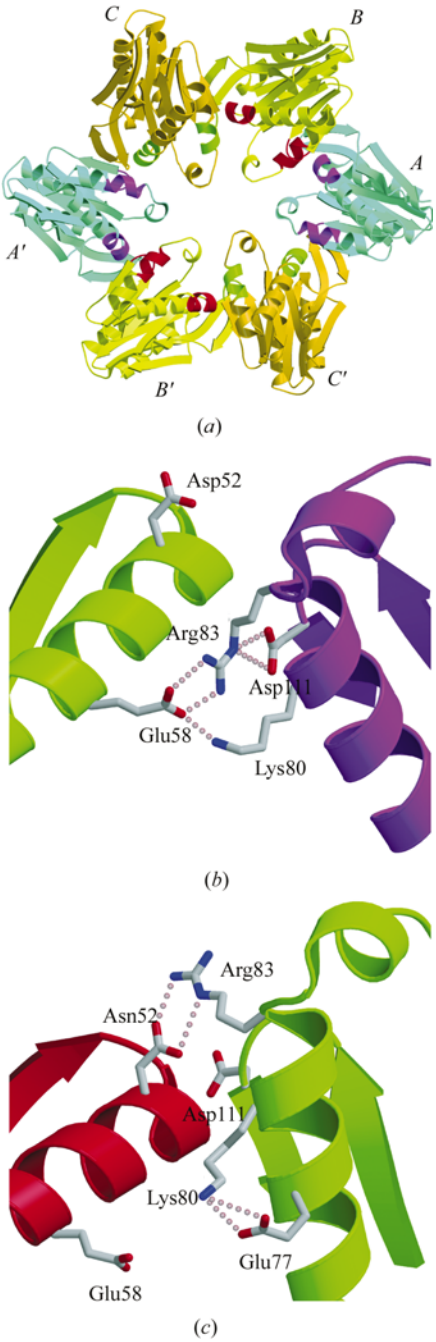

Figure 1
Quasi-equivalent subunit interactions within HslV. (*a*) Ribbon drawing of one hexamer, looking down the pseudo-sixfold axis. Subunits related by crystallographic twofold rotation are shown in identical colors and denoted with a prime. Regions on the apical helices which reveal differences in subunit–subunit interactions are highlighted: magenta on cyan for subunit *A*; red on yellow for subunit *B*; green on gold for subunit *C*. (*b*) Interactions between subunits *C* and *A*, using same color coding as in (*a*). (*c*) Interactions between subunits *B* and *C*. Figs. 1 and 2(*b*) were produced with *MOLSCRIPT* (Kraulis, 1991) and Fig. 2(*a*) was produced with *BOBSCRIPT* (Esnouf, 1997, 1999); all figures were rendered with *Raster3D* (Merritt & Bacon, 1997).

in tertiary fold to the β-subunits. In the proteasome, therefore, the presence of Mg^{2+} in a subunit at the sites equivalent to the monovalent ion-binding site of HslV is associated with catalytic activity, either of the subunit itself or of a neighboring subunit related through a 'β-*trans*-β' interaction.

We have attempted to replace the monovalent ion in our HslV crystals with Mg^{2+}, but all efforts to exchange Mg^{2+} for Na^{+} resulted in disordering of the crystals. However, in crystals of the *H. influenzae* HslUV complex which have been adapted to a mother liquor that includes 1 *M* $Mg(OAc)_2$, we see a significant positive peak at this site in $F_o - F_c$ difference Fourier maps, which probably arises from a hydrated Mg^{2+} ion, although the resolution of the data (3.1 Å; Souza & McKay, unpublished results) is not sufficient to resolve the ligand structure. We presume this site can bind monovalent cations and Mg^{2+} interchangeably.

Binding of the HslU chaperone to HslV is a prerequisite for significant peptidase activity; HslU is an allosteric activator of the HslV protease. We have measured the hydrolytic activity of the HslUV complex on Z-Gly-Gly-Leu-AMC in the presence of Mg^{2+} and nucleotide (both ATP and ADP) and find that K^{+} has a minor inhibitory effect, while EDTA abolishes activity. We have also found by gel filtration (data not shown) that Mg^{2+} and K^{+} at concentrations of 5 m*M* and ~1 *M*, respectively, have interchangeable effects in stabilizing the complex between HslU and HslV. Other investigators have measured the activity of *E. coli* HslUV and have reported a complex behavior in which K^{+} has little effect on peptidase activity in the presence of ATP and 5 m*M* Mg^{2+}, but is stimulatory in the presence of the non-hydrolyzable analog AMPPNP (Huang & Goldberg, 1997). Thus, it is clear that both monovalent and divalent ions modulate the assembly and peptide-hydrolysis activity of the HslUV complex in a manner that cannot be attributed solely to the interaction of Mg^{2+} with ATP and ADP on HslU. One mechanism through which ion binding to HslV might affect the peptidase activity of the HslUV complex is through perturbation of the geometry and electrostatic environment of the protease active site by ions differing by a unit in charge and a few tenths of an ångström in ionic radius. An alternative mechanism is that ions binding to HslV may stabilize the complex between HslV and HslU through allosteric interactions. Currently available data do not discriminate between these alternatives. Mg^{2+} is thought to be a necessary cofactor of ATP for the HslU-dependent protease activity and hence it is routinely included in activity assays. As a consequence, the necessary inclusion of Mg^{2+} in assays testing the effect of monovalent ions on the peptidase activity of HslV obscures the interpretation of results, since Mg^{2+} ions appear to bind HslV interchangeably with monovalent ions.

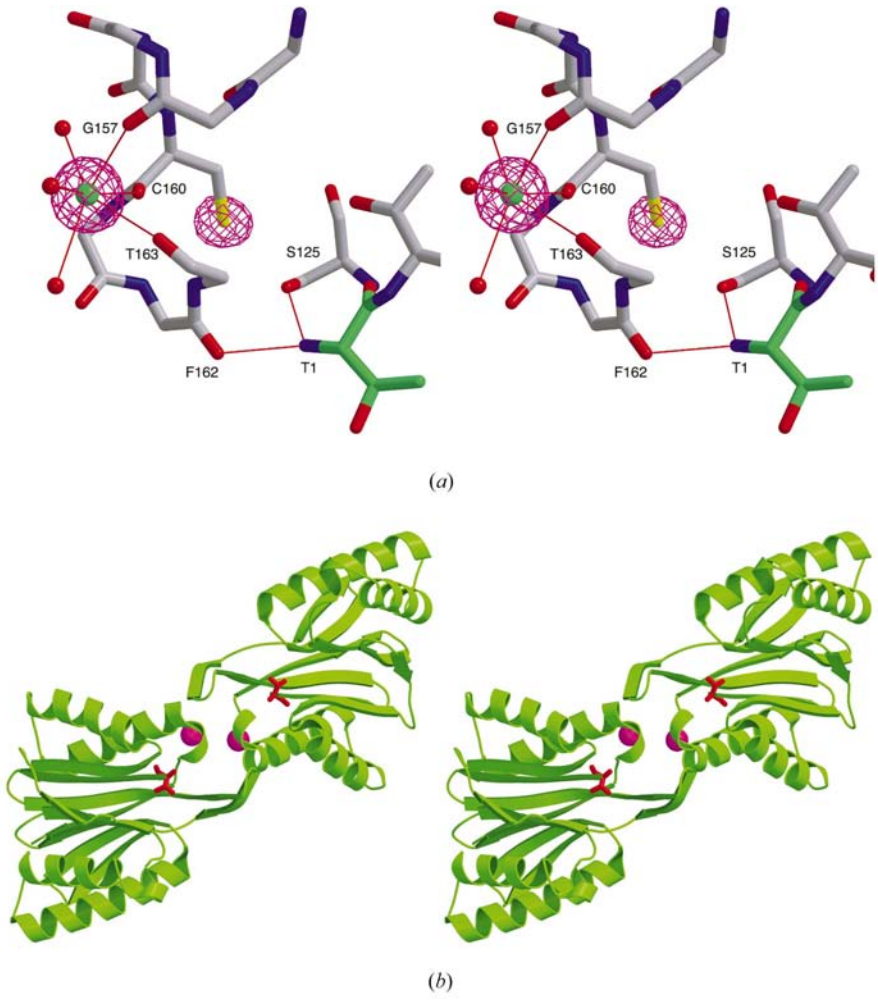

Figure 2
The monovalent ion-binding site. (*a*) Anomalous difference Fourier computed with data from the K^{+}-bound crystal, contoured at 6σ, showing peaks for the K^{+} ion and the S atom of Cys160. Interactions with K^{+} ion and active-site Thr1 (green) are shown; for clarity, most amino-acid side chains have been omitted. (*b*) Two HslV subunits, showing relationship of ion-binding sites to active site Thr1. K^{+} ions are magenta; the active-site Thr1 residue is red. One subunit from each hexamer of the dodecamer is shown; the view is perpendicular to the pseudo-sixfold axis, which is approximately vertical.

3.3. Summary

The high-resolution structures of HslV in this crystal form provide an example of quasi-equivalent interactions between subunits in a non-viral oligomeric assembly. Whether the conformational variability within subunits that gives rise to the asymmetry is intrinsic to the HslV dodecamer in solution or is induced by crystal-packing interactions remains undetermined. In either case, the structure reveals a structural malleability of the dodecamer that may be a requisite for the conformational changes that HslV undergoes when it binds HslU.

The structures also reveal monovalent ions bound with octahedral coordination at a site occupied by a Mg^{2+} ion in some subunits of the yeast proteasome. We presume that monovalent and divalent ions can bind interchangeably at this site. The realisation that K^{+} and Na^{+} ions may compete with Mg^{2+} ions at this site and that they may further affect the proteolytic activity of HslV through allosteric interactions with the catalytic Thr1 residue should clarify the interpretation of future activity measurements of the HslUV protease complex.

This work was supported by grant NIH-GM39928 to DBM. Portions of this research were carried out at the Stanford Synchrotron Radiation Laboratory, a national user facility operated by Stanford University on behalf of the US Department of Energy, Office of Basic Energy Sciences. The SSRL Structural Molecular Biology Program is supported by the Department of Energy, Office of Biological and Environmental Research, by the National Institutes of Health, National Center for Research Resources, Biomedical Technology Program and the National Institute of General Medical Sciences.

References

Bochtler, M., Ditzel, L., Groll, M. & Huber, R. (1997). *Proc. Natl Acad. Sci. USA*, **94**, 6070–6074.

Bochtler, M., Hartmann, C., Song, H. K., Bourenkov, G. P., Bartunik, H. D. & Huber, R. (2000). *Nature (London)*, **403**, 800–805.

Brunger, A. T., Adams, P. D., Clore, G. M., DeLano, W. L., Gros, P., Grosse-Kunstleve, R. W., Jiang, J. S., Kuszewski, J., Nilges, M., Pannu, N. S., Read, R. J., Rice, L. M., Simonson, T. & Warren, G. L. (1998). *Acta Cryst.* D**54**, 905–921.

Chuang, S. E., Burland, V., Plunkett, G., Daniels, D. L. & Blattner, F. R. (1993). *Gene*, **134**, 1–6.

Cromer, D. T. (1974). *International Tables for X-ray Crystallography Volume IV. Revised and Supplementary Tables to Volumes II and III*, edited by J. A. Ibers & W. C. Hamilton, pp. 149–153. Birmingham, England: The Kynoch Press.

Esnouf, R. M. (1997). *J. Mol. Graph.* **15**, 132–134.

Esnouf, R. M. (1999). *Acta Cryst.* D**55**, 938–940.

Glusker, J. P. (1991). *Adv. Protein Chem.* **42**, 1–76.

Groll, M., Ditzel, L., Löwe, J., Stock, D., Bochtler, M., Bartunik, H. D. & Huber, R. (1997). *Nature (London)*, **386**, 463–471.

Huang, H. & Goldberg, A. L. (1997). *J. Biol. Chem.* **272**, 21364–21372.

Jones, T. A., Zhou, J. Y., Cowan, S. W. & Kjeldgaard, M. (1991). *Acta Cryst.* A**47**, 110–119.

Kessel, M., Wu, W., Gottesman, S., Kocsis, E., Steven, A. C. & Maurizi, M. R. (1996). *FEBS Lett.* **398**, 274–278.

Kleywegt, G. J. & Jones, T. A. (1997). *Methods Enzymol.* **277**, 525–545.

Kraulis, P. (1991). *J. Appl. Cryst.* **24**, 946–950.

Lee, B. & Richards, F. M. (1971). *J. Mol. Biol.* **55**, 379–400.

Löwe, J., Stock, D., Jap, B., Zwickl, P., Baumeister, W. & Huber, R. (1995). *Science*, **268**, 533–539.

Luzzati, V. (1952). *Acta Cryst.* **5**, 802–810.

Merritt, E. A. & Bacon, D. J. (1997). *Methods Enzymol.* **277**, 505–524.

Navaza, J. (1994). *Acta Cryst.* A**50**, 157–163.

Otwinowski, Z. & Minor, W. (1997). *Methods Enzymol.* **276**, 307–326.

Rohrwild, M., Pfeifer, G., Santarius, U., Muller, S. A., Huang, H. C., Engel, A., Baumeister, W. & Goldberg, A. L. (1997). *Nature Struct. Biol.* **4**, 133–139.

Seol, J. H., Yoo, S. J., Shin, D. H., Shim, Y. K., Kang, M. S., Goldberg, A. L. & Chung, C. H. (1997). *Eur. J. Biochem.* **247**, 1143–1150.

Sousa, M. C., Trame, C. B., Tsuruta, H., Wilbanks, S. M., Reddy, V. S. & McKay, D. B. (2000). *Cell*, **103**, 633–643.

Wang, J., Song, J. J., Franklin, M. C., Kamtekar, S., Im, Y. J., Rho, S. H., Seong, I. S., Lee, C. S., Chung, C. H. & Eom, S. H. (2001). *Structure*, **9**, 177–184.

Yoo, S. J., Seol, J. H., Seong, I. S., Kang, M. S. & Chung, C. H. (1997). *Biochem. Biophys. Res. Commun.* **238**, 581–585.